Indian Journal of Engineering & Materials Sciences
Vol. 27, June 2020, pp. 783-788

Average austenite grain size evolution simulation during multi-pass shape metal hot rolling process

He Qingqiang*, Zhu Han, Liu Jianguo, Chai Wanli, Geng Chunli & Zhao Junyou
School of Mechanical Engineering, China University of petroleum, Qingdao 266580, P.R. China

Received:06 September 2017 ; Accepted:25 June 2018

Constitutive equations describing the flow stress of Q235 steel undergoing hot plastic deformation have been developed by integrating the microstructure models and exponential flow stress models presented in literatures, in which the microstructure models parameters have been re-determined based on the related experiments carried out on cylindrical specimens of the Q235 steel. Therefore, the integrated constitutive equations are capable of calculating the evolution of austenite grain size and investigating the effects of average austenite grain size on the flow stress of Q235 steel during hot deformation. A three-dimensional thermo-mechanically coupled FEM simulation of an 11-pass H-shape metal roughing rolling process with the austenite grain size evolution taken into account have been carried out to verify the rationality of roll pass schedule. The accuracy of the integrated constitutive equations has been preliminary validated by the comparisons between measured and the calculated values of rolling force.

Keywords: Hot rolling, FEM simulation, Austenite grain size evolution

1 Introduction

The problem of thermo-mechanical-microstructure modeling of metal behaviour during hot deformation has become very popular in the last few years. Phaniraj presented[1] their research results on modeling of hot strip mill using finite element method coupled with the microstructure evolution. Glowacki presented[2] a generalized plane-strain (GPS) approach for fast simulation of multi-pass shape rolling. Liu and Lin developed[3] a set of mechanism-based unified viscoplastic constitutive equations and numerical procedures to simulate multi-pass rolling with two-dimensional finite element method. Bontcheva and Petzov presented[4] an axial-symmetric approach for numerical simulation of die forging using the finite element code MARC. Bontcheva and Petzov[5] simulated the microstructure evolution of stainless 304 steel in hot rolling and consequent cold torsion with evaluating the aggregate austenite-marten site flow stress. Lin and Dean introduce their techniques for the development of functions of physical variables and coupling of the variables within visco-plastic material models to form a set of unified constitutive equations[6]. Predicting of mechanical properties[2,6] of the products was also presented. Grass presented[7] their results of a five-pass stretch rolling process in fully three-dimensional thermo-mechanically coupled FEM-simulation. Benson and Okazawa developed[8] an Eulerian contact formulation and machining was chosen as the model problem for investigating the formulations because its new free surface generation makes it a natural application for the Eulerian finite element formulations. Eulerian-formulation finite element method was used to describe granular flow in hopper to avoid difficulties caused by large plastic deformation[9].

The dislocation density distribution was computed using a crystal plasticity finite element method framework and the primary recrystallization was modelled by means of a cellular automaton approach[10]. The distribution of equivalent and shear strain of aluminium alloy plate during snake hot rolling was studied through coupled thermo-mechanical finite element models[11]. The evolutionary mechanism of microstructure with periodic thermal parameters during ACDR process was established through the numerical simulation[12].

Based on the microstructure models [13] developed by Hodgson, the content of this presented work is mainly concentrated on parameters determination of the mechanism-based constitutive equations for the Q235 steel undergoing hot plastic deformation, and the three-dimensional finite element simulation of multi-pass H-shape metal rolling process implemented by special

*Corresponding author (E-mail: heqingqiang_upc@163.com)

approach[14,15] presented by the author. The evolution of austenite grain size and the hot billet temperature during rolling and the inter-pass rolling time was investigated to preliminary verify the roll pass schedule rationality of an 11-pass H-shape metal roughing rolling. The measured values of rolling force and the calculated ones were also presented.

2 Modelling of the Metal Hot Plastic Deformation Process

The main chemical composition of the Q235 steel is listed in Table 1.

The material flow stress σ_y is assumed to be dependent on equivalent plastic strain ε_p^{eq}, equivalent plastic strain rate ε_{rp}^{eq}, transition Kelvin temperature of billet T and current average austenite grain size D. It was defined as eqs 1 and 2:

$$\sigma_y(\varepsilon_p^{eq}, T, \varepsilon_{rp}^{eq}, D) = A\varepsilon^n, \varepsilon \le \varepsilon_{cr} \quad \ldots (1)$$

$$\sigma_y(\varepsilon_p^{eq}, T, \varepsilon_{rp}^{eq}, D) = A\varepsilon^n(1 - X_{rx}) + \sigma_s X_{rx}, \varepsilon > \varepsilon_{cr} \quad \ldots (2)$$

The microstructure models developed by Hodgson[13] were assumed applicable for the Q235 steel and integrated into the flow stress model with local modifications. The parameters determined for Q235 steel were listed in Table 2. The equations were then implemented into FEM solver *ABAQUS/Explicit*

Table 1 — Chemical compositions of Q235 steel.

C(%)	Mn(%)	Si(%)	S(%)	P(%)
0.12~0.20	0.30~0.70	0.12~0.30	≤0.045	≤0.045

Table 2 — Parameters in material flow stress equation determined for the Q235 steel.

Parameter	Equation or expression	units
Material dependent constant	$A=1.856Z^{0.144}$	*Mpa*
Material dependent constant	$n=log(\sigma_0/A)/log(0.002)$	
Initial yield stress	$\sigma_0=3.348Z^{0.16}$	*Mpa*
Steady flow stress	$\sigma_s=1.608Z^{0.147}$	*Mpa*
Recrystallization fraction		
SRX	$X_s=1-exp(-0.693(t_s/ t_{0.5}^s))$	
DRX	$X_d=1-exp(-0.8(\varepsilon_p^{eq} -\varepsilon_{cr})/\varepsilon_{pk})^{1.4})$	
MDRX	$X_{md}=1-exp(-0.693(t_{md}/ t_{0.5}^{md})^{1.5})$	
Time for 50% recrystallizaion		*s*
SRX	$t_{0.5}^s=2.3E-15(\varepsilon_p^{eq})^{-2.5}D^2exp(230,000/RT)$	
MDRX	$t_{0.5}^{md}=1.1Z^{-0.8}D^2exp(230,000/RT)$	
Current average austenite grain size		*μm*
SRX	$D_s=343D_0^{0.4}(\varepsilon_p^{eq})^{-0.5}exp(-450,000/RT)$	
DRX	$D_d=2.6E4Z^{-023}$	
MDRX	$D_{md}=2.6E4Z^{-023}D_d^{0.99}$	
Partial recrystallizaion	$D_{j+1}=D_{rxj}X_{rx}+D_j(1-X_{rx})$	
Grain growth size		*μm*
SRX, $X_s \ge 0.99$	$(D_{st}^{gr})^7=(D_p)^7+1.5E27exp(-400,000/RT)\ t_{sg}$	
$t_{sg} \ge 1$	$(D_{st}^{gr})^2=(D_p)^2+4.0E7exp(-113,000/RT)\ t_{sg}$	
$t_{sg} < 1$	$(D_{mdt}^{gr})^7=(D_p)^7+8.2E25exp(-400,000/RT)\ t_{mdg}$	
MDRX, $X_d \ge 0.99$	$(D_{mdt}^{gr})^2=(D_p)^2+1.2E7exp(-113,000/RT)\ t_{mdg}$	
$t_{mdg} \ge 1$		
$t_{mdq} < 1$		
Time for grain growth		
SRX	$t_{sg}=t-4.23t_{0.5}^s$	
MDRX	$t_{mdq}=t-2.65t_{0.5}^{md}$	
Time measured from the moment as soon as SRX or DRX is complete	t	*s*
Austenite grain size during heating treatment	$D_{sht}=(C^3+Bexp(200,000/RT)t_{ht})^{1/3}$	*μm*
Material dependent constant	$B=1.56E12$	
Material dependent constant	$C= 30$	*μm*
Time for heating treatment	t_{ht}	*s*
Peak strain	$\varepsilon_{pk}=0.00154Z^{0.206}$	
Crtical strain	$\varepsilon_{cr}=(5/6)\ \varepsilon_{pk}$	
Zener-Hollomon parameter	$Z=\varepsilon_{rp}^{eq}\ exp(300,000/RT)$	
Gas constant	$R=8.314$	*J/(mol·K)*
Transition Kelvin temperature of billet	T	*K*
Equivalent plastic strain rate	$\varepsilon_{rp}^{eq}=\int d\varepsilon_{rp}^{eq}$	
Current equivalent plastic strain	$\varepsilon_p^{eq}=\int d\varepsilon_p^{eq}+\varepsilon_{ap}^{eq}$	
Accumulated equivalent plastic strain	$\varepsilon_{ap}^{eq}{}_{j+1}=\varepsilon_p^{eq}{}_j+\varepsilon_p^{eq}(1-X_{rx})$	

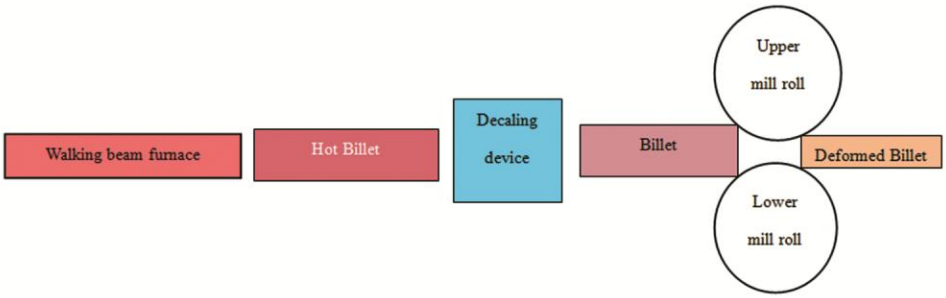

Fig. 1 — Schematic drawing of reversing mill rolling of H-shape metal.

through the *VUMAT* subroutine for simulation of multi-pass shape rolling process.

3 Simulation of the H-Shape Metal Multi-Pass Rolling

Simulations of the rolling process of H-shape metal H400×200×8/13 would be investigated in this work. The billet has a 320×410 mm^2 cross section and 5000 mm in length. The rolling schedule includes roughing and finishing rolling passes, and a schematic drawing illustrating the production process was shown as Fig. 1. In this presented work simulations of the rolling force and billet temperature during roughing rolling passes as well as the inter-pass time would be considered. According to the roll pass schedule, 11 passes shaped by four different gauges with predesigned rolling parameters would be applied to the roughing rolling process. A schematic drawing of the gauges geometry without dimensions was shown in Fig. 2. The first four passes are rolled in the gauge 1, and the next four passes are rolled in the gauge 2, two passes in gauge 3, and the last one pass in gauge 4. The rolling schedules were listed in much detail in Table 3.

Considering the forming conditions and geometrical symmetry, only a half of the billet was modelled and simulated in ABAQUS solver for time saving.

The initial temperature of the hot billet is 1310 °C, and the initial austenite grain size in the billet is 390 μm. The heat transfer coefficient between the rollers and hot billet, listed in Table 4, was assumed to be dependent on the minimum gap distance between the two surfaces, and the friction coefficient between rollers and billet was defined as $f=1.05-5\times10^{-4}\times T-5.6\times10^{-2}\times v$, where T is the current temperature of billet and the v is the rolling velocity. The equation was implemented into the *ABAQUS/Explicit* solver through user-defined subroutine *VFRIC*.

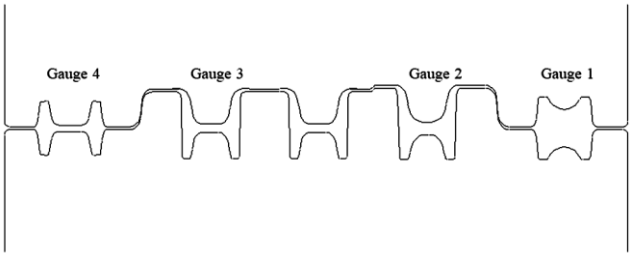

Fig. 2 — Schematic drawing of the gauges geometry without dimensions.

Table 3 — Rolling schedule for an 11-pass H-shape metal hot roughing rolling processes.

Pass No.	Gauge	Roll Gap/mm	Rotate Speed of Rollers /RPM	Velocity of billet /MPM
1	Gauge1-1	258	42.4	120.0
2	Gauge1-2	201	34.0	96.0
3	Gauge1-3	144	34.0	96.0
4	Gauge1-4	108	40.9	96.0
5	Gauge2-1	84	40.9	120.0
6	Gauge2-2	61	61.3	120.0
7	Gauge2-3	47	61.3	180.0
8	Gauge2-4	38	61.3	180.0
9	Gauge3-1	32	50.1	150.0
10	Gauge3-2	24	60.1	180.0
11	Gauge4	18	59.8	180.0

Table 4 — The value of heat transfer coefficient.

Heat transfer coefficient value / W/(m·K)	Gap distance /mm
35.5	0
10	0.1
0	0.5

4 Results and Discussion

SDV1 is an inner parameter standing average austenite grain size in the presented work. Figure 3 shows the average grain size distribution of austenite, calculated by three different element meshing size, in the steady state elements set of the billet in the first roughing rolling pass.

Figure 3(a) are results based on the rough finite elements, in which the element size was set to

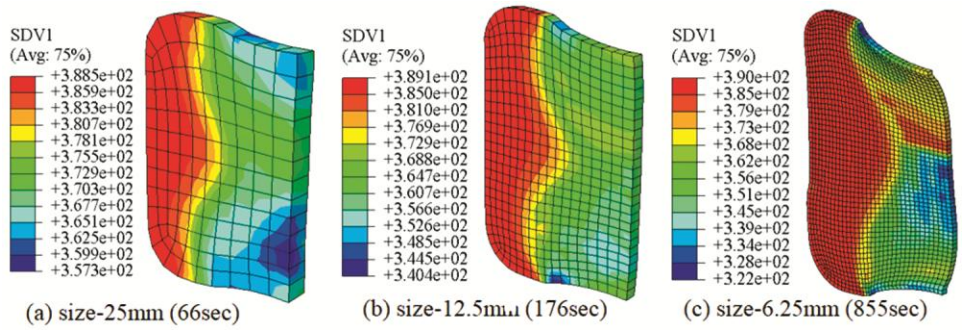

Fig. 3 — Austenite grain size distribution in the steady state elements set in the first roughing rolling pass (a) size-25mm (66sec), (b) size-12.5mm (176sec) and (c) size-6.25mm (855sec).

25 mm, and calculation time was about 66 seconds. In Fig. 3(b & c) the element sizes reduced to 1/2 and 1/4 of rough finite elements respectively, the calculation time was increased to 176 and 855 seconds, about 2.7 and 13 times the calculation time of rough finite elements. The grain size distribution and the maximum grain size are the same under three element meshing size, only the minimum austenite grain size decreased with mesh refinement, and the decreasing amplitude is about 5%.

Considering the computation time and the accuracy of calculation, the upper limit of the element size in the billet section is set to no more than 12mm, and adjusted with the shape change of the billet section. In addition, in order to reduce the total number of finite elements, the finite element size of the normal direction of billet section is set to 25mm.

Figure 4 shows the average grain size distribution of austenite at the end of the 11th roughing rolling pass. It shows that the minimum austenite grain size is about 34 μm at the end of the 11th pass, and the austenite grain size at the billet web are much refined and homogeneous than those in the flange. Therefore, in the following finishing rolling process the main aim of the schedule designer is to refine the austenite grain in the flange. However, it is difficult to fulfil this aim only by their operational experience, and it is very expensive to carry out experiments because of very high machinery costs and loss of production. Therefore, in order to reduce the cost of designing the new hot rolling schedule, numerical analysis could be carried out before actual production.

Figure 5 presents the results of calculated billet temperature distribution in the last roughing rolling pass. It shows that an initially homogeneous temperature becomes in-homogeneous with an temperature difference about 340 °C at the end of the rolling process.

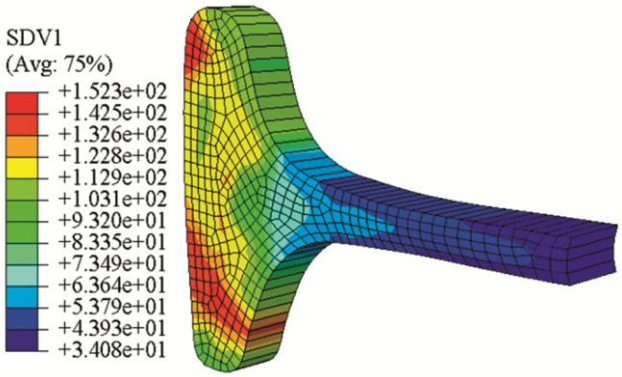

Fig. 4 — The calculated austenite grain size distribution in the steady state elements set of the billet in the 11th roughing rolling pass.

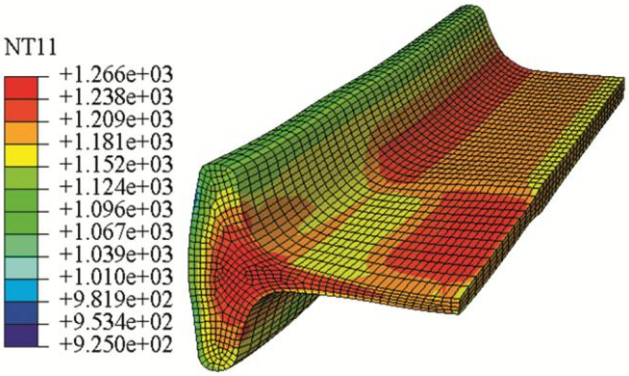

Fig. 5 — Calculated temperature distribution in billet in the 11th roughing rolling pass.

SDV6 is another inner parameter standing for the dynamic recrystallization volume fraction in this presented work. The predicted distributions of dynamic recrystallization volume fraction in the last roughing rolling pass was shown in Fig. 6. It shows that the maximum volume fraction of dynamic recrystallization occurs at the regions undergoing the biggest plastic deformation.

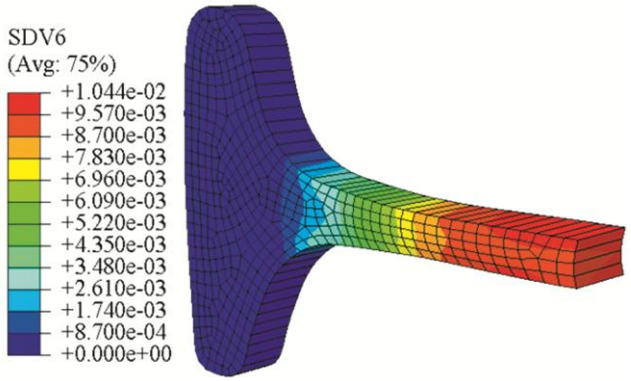

Fig. 6 — Distributions of dynamic recrystallization volume fraction in the 11th roughing rolling pass.

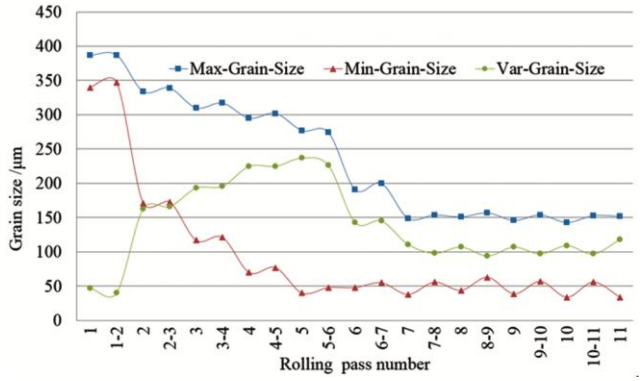

Fig. 7 — Evolution of the maximum, minimum and variance of austenite grain size.

Figure 7 shows the evolution of the maximum, minimum and variance of austenite grain size in the billet during the whole rolling passes, including the inter-pass rolling process. It was shown that the austenite grain size changes from the initial value about 390 μm to the minimum value about 30 μm at the end of rough rolling process, and during the inter-pass time, the austenite grain size has a slight increase. However, after the 5th rolling pass the minimum austenite grain size is fluctuates around 50 μm.

Figure 8 shows the changing of the maximum, minimum and variance of billet temperature during the whole rolling passes. It can be seen that the minimum temperature changes from the initial value about 1150 °C to 930 °C, and during the inter-pass time the billet temperature has a slight increase because the heat conduction within the hot billet. It also found that except for the last few passes, the maximum billet temperature is almost unchanged throughout the roughing rolling process because of the heat generated by the big plastic deformation.

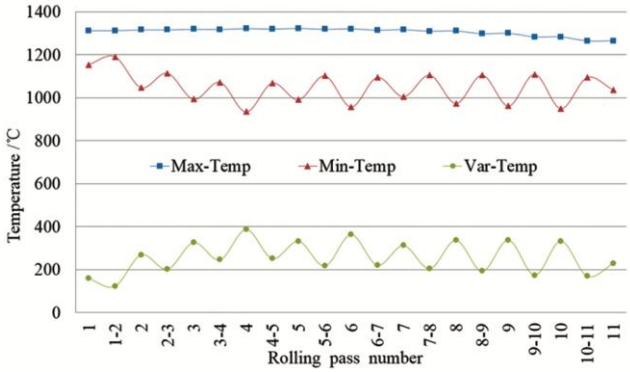

Fig. 8 — Evolution of the maximum, minimum and variance of hot billet temperature.

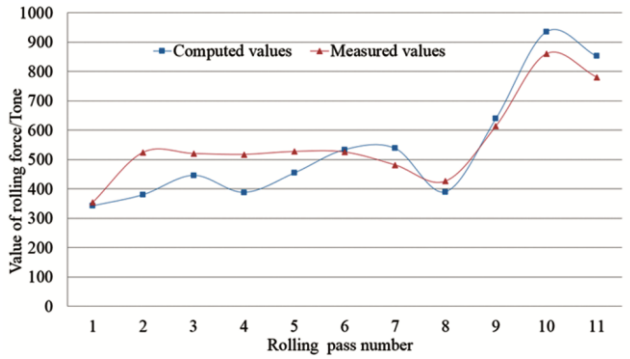

Fig. 9 — Comparison between the calculated and measured mill load values.

Comparison between calculated and measured values of mill load during the industrial rough rolling process of the 11-pass H-shape metal was presented in Fig. 9. The similarity in measured and calculated values preliminary shows a good predictive ability of the constitutive models for the Q235 steel developed in this presented work.

5 Conclusions

The FEM simulation of multi-pass H-shape metal rolling process is a three-dimensional problem, so the microstructure evolution and their effects on the material flow were hard to determine without the utilization of numerical modelling and simulation software. The set of unified constitutive equations presented in this work enables to predict distribution of billet temperature and average austenite grain size evolution of the Q235 steel during the rolling process and the inter-pass time, which is very helpful for engineers working on roll pass design. By using the developed materials model and the FE procedures, the evolution of austenite grain size during multi-pass hot rolling process could be investigated to optimize the

hot rolling schedule, reducing the number of experiments and the cost of expensive industrial tests.

Acknowledgment

The researches were supported by the Shandong Provincial Natural Science Foundation, China (ZR2019MEM038) and the Fundamental Research Funds for the Central Universities (18CX02090A), their supports are greatly acknowledged.

References

1 Phaniraj M P, *J Mater Process Tech*, 178 (2006) 388.
2 Liu Y & Lin J, *J Mater Process Tech*, 144 (2003) 723.
3 Glowacki M, *J Mater Process Tech*, 168 (2005) 336.
4 Bontcheva N & Petzov G,*Comp Mater Sci*, 28 (2003) 563.
5 Bontcheva N & Petzov G, *Comp Mater Sci*, 34 (2005) 377.
6 Lin J & Dean T A, *J Mater Process Tech*, 167 (2005) 354.
7 Grass H , Krempaszky C, Reip T & Werner E, *Comp Mater Sci*, 28 (2003) 469.
8 Benson D J & Okazawa S, *Comput Method Appl M*, 193 (2004) 4277.
9 Zheng Q J & Yu A B, *Chem Eng Sci*, 129 (2015) 49.
10 Haase C, *Acta Mater*, 100 (2015) 155.
11 Zhang T, Wu Y X & Gong H, *J Cent South Univ*, 24 (2017) 296.
12 Zheng Y, Liu D & Yang Y Y, *J Alloy Compd*, 735 (2018) 996.
13 Hodgson P D, *J Mater Process Tech*, 60 (1996) 27.
14 He Q Q & Sun J, *J South Univ of Tech*, 38 (2010) 144.
15 He Q Q & Sun J, *Finite Elem Anal Des*, 76 (2013)13.